JOURNAL OF MATERIALS SCIENCE **35** (2000) 3539 – 3546

Comparative study of grain growth behavior from a supercooled liquid region of $Zr_{65}Cu_{27.5}Al_{7.5}$ and $Zr_{65}Cu_{35}$ metallic glasses

J. SAIDA, M. MATSUSHITA, C. LI
Inoue Superliquid Glass Project, ERATO, Japan Science and Technology Corporation (JST), Sendai 982-0807, Japan
E-mail: jsaida@sendai.jst.go.jp

A. INOUE
Inoue Superliquid Glass Project, ERATO, Japan Science and Technology Corporation (JST), Sendai 982-0807, Japan; Institute for Materials Research, Tohoku University, Sendai 980-8577, Japan

The grain growth behavior of a Zr_2Cu crystalline phase from a supercooled liquid region of $Zr_{65}Cu_{27.5}Al_{7.5}$ and $Zr_{65}Cu_{35}$ metallic glasses was examined as a function of annealing time, t_a at various temperatures. Since no distinct change of constitution and strain in Zr_2Cu phase is seen, the grain size calculated from a line-broadening of X-ray diffraction peak by Scherrer's formula can be used. The calculated grain size is in agreement with that obtained by transmission electron microscopy observation. The curve of grain size with t_a is parabolic. The grain growth in $Zr_{65}Cu_{35}$ takes place at lower temperature and its rate is extremely larger as compared with those of $Zr_{65}Cu_{27.5}Al_{7.5}$. These differences are originated from the suppression of growth of Zr_2Cu by Al atom, which retards the diffusion of Cu owing to the primary precipitation of ZrAl in $Zr_{65}Cu_{27.5}Al_{7.5}$. The formation of ZrAl may be attributed to the strong chemical affinity between Al and Zr. The activation energies for grain growth of 115 kJ mol^{-1} for $Zr_{65}Cu_{27.5}Al_{7.5}$ and 363 kJ mol^{-1} for $Zr_{65}Cu_{35}$ are obtained by the Arrhenius plot of grain growth rate against a reciprocal of temperature. These activation energies reflect the kind and/or magnitude of diffusion atoms during the grain growth. © *2000 Kluwer Academic Publishers*

1. Introduction

Since new metallic glasses with a wide supercooled liquid region before crystallization were found in the Mg- [1, 2], La- [3], Pd- [4], Ti- [5] and Zr-based [6] systems, great attention has been paid to the mechanism for the high stability of supercooled liquid in their special alloy systems. Among these metallic glasses, the Zr-TM-Al (TM is a transition metal) alloys are particularly interesting because they have an extremely wide supercooled liquid region exceeding 100 K [7]. The supercooled liquid region is defined by the temperature interval between the glass transition temperature T_g and crystallization temperature T_x. In the Zr-based ternary alloy system, $\Delta T_x (\Delta T_x = T_x - T_g)$ shows a maximum value of about 90 K for the $Zr_{65}Cu_{27.5}Al_{7.5}$ alloy [8]. Structural analysis [9], thermal stability [10] and crystallization kinetics [11, 12] in supercooled liquid and amorphous states of the $Zr_{65}Cu_{27.5}Al_{7.5}$ metallic glass have already been reported and the appearance of the wide supercooled liquid region has been attributed to the difficulty of precipitation of crystalline phases resulting from the large solid-liquid interfacial energy and the suppression of growth due to the necessity of long-range redistribution of Al at the solid-liquid interface [13]. The authors reported that metastable ZrAl and unknown phases are observed at the initial crystallization stage, in addition to a main phase of b.c.t. $Zr_2(Cu, Al)$ [14]. The lattice spacing and grain size of Zr_2Cu changed significantly with disappearing ZrAl, implying that Al has an important role in the growth reaction of Zr_2Cu. However, little is known about the grain growth behavior of a main crystalline phase at the initial crystallization process where is closely related with the stabilization of the glassy state. This study is intended to examine the grain growth behavior of the Zr_2Cu phase in the glassy $Zr_{65}Cu_{27.5}Al_{7.5}$ alloy in comparison with those in $Zr_{65}Cu_{35}$ in order to clarify the effect of Al on the grain growth of crystalline phase, and to investigate the reason for the high stability of the supercooled liquid against crystallization.

2. Experimental procedure

A ternary $Zr_{65}Cu_{27.5}Al_{7.5}$ alloy and a binary $Zr_{65}Cu_{35}$ alloy were examined in the present study. The prealloyed ingots were prepared by arc-melting a mixture of pure metals in a purified Ar atmosphere. The composition is given in nominal atomic percent. The amorphous alloy ribbon was prepared by a single roller melt-spinning technique in an Ar atmosphere. The structure and thermal properties of the as-quenched sample were examined by X-ray diffractometry with Cu K_α radiation and differential scanning calorimetry (DSC) with a heating rate of 0.67 K s^{-1}, respectively. The amorphous ribbon was annealed with various times in a temperature range of 700 K to 730 K for $Zr_{65}Cu_{27.5}Al_{7.5}$ and 640 K to 660 K for $Zr_{65}Cu_{35}$, respectively. The grain size was measured by X-ray line-broadening using Scherrer's formula [15] and transmission electron microscopy (TEM) observation for the isothermal annealed samples.

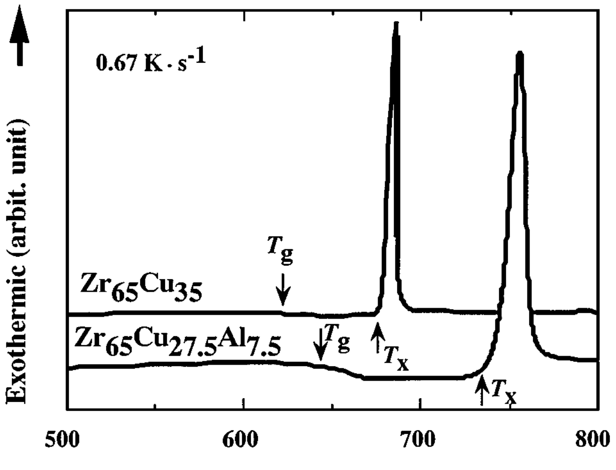

Figure 1 Differential scanning calorimetry (DSC) curves of an as-prepared $Zr_{65}Cu_{27.5}Al_{7.5}$ and $Zr_{65}Cu_{35}$ metallic glasses.

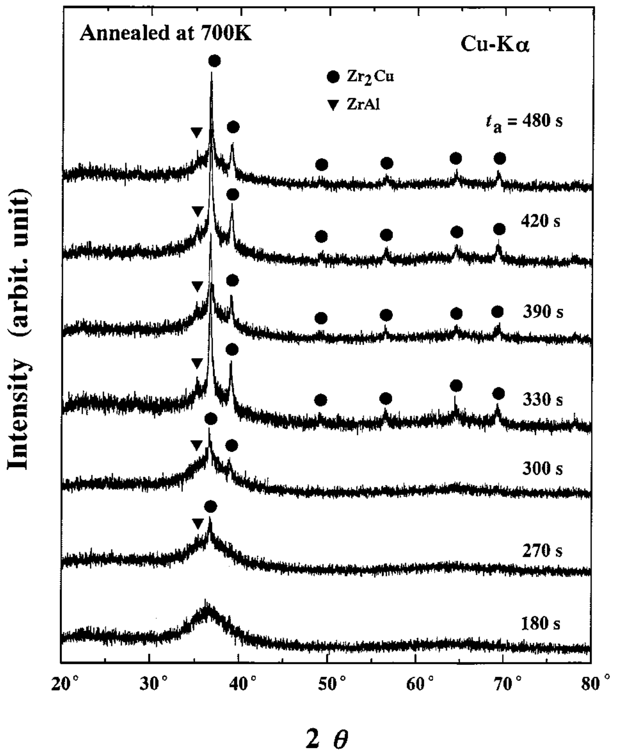

Figure 2 X-ray diffraction patterns of the annealed samples with various times at 700 K for the $Zr_{65}Cu_{27.5}Al_{7.5}$ metallic glass.

3. Results

Fig. 1 shows DSC curves of the $Zr_{65}Cu_{27.5}Al_{7.5}$ and $Zr_{65}Cu_{35}$ metallic glasses. The glass has a wide supercooled liquid region with $\Delta T_x = 85$ K for $Zr_{65}Cu_{27.5}Al_{7.5}$ and 54 K for $Zr_{65}Cu_{35}$, respectively. The T_g and T_x are determined to be 646 K and 731 K, respectively, for the former alloy and 624 K and 678 K, respectively, for the latter alloy. Fig. 2 shows the change in X-ray diffraction patterns of the $Zr_{65}Cu_{27.5}Al_{7.5}$ alloy with annealing time, t_a at 700 K. A ZrAl phase is seen in addition to the main Zr_2Cu phase. The authors have previously reported that the ZrAl phase is metastable and the grain growth of Zr_2Cu is enhanced with a deconvolution of ZrAl phase [14]. In this study, the grain growth in the $Zr_{65}Cu_{27.5}Al_{7.5}$ alloy was examined under the coexistence of Zr_2Cu and ZrAl. On the other hand, it is well known that the $Zr_{65}Cu_{35}$ alloy crystallizes through the precipitation of a single Zr_2Cu phase. The intensity of the X-ray diffraction peaks of Zr_2Cu phase increases with increasing annealing time, while the width of line-broadening appears to decrease, suggesting that the grain growth takes place. As the line-broadening consists of three factors of grain size, constituent and strain, the influence of constituent and strain of the Zr_2Cu phase should be considered to evaluate a grain size. The change in the lattice spacing of

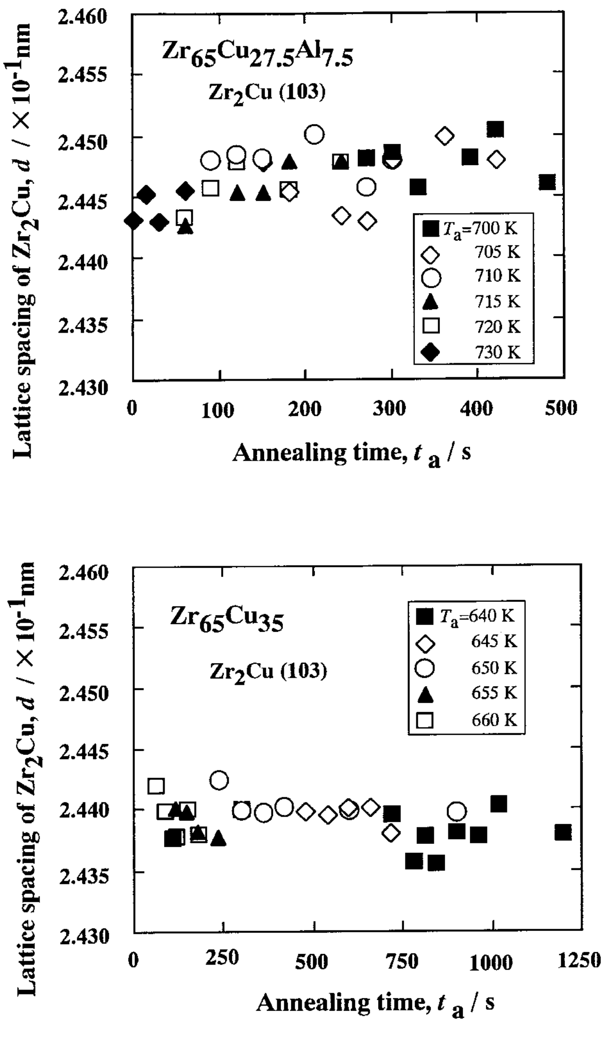

Figure 3 Change in the lattice spacing of Zr_2Cu (103) with annealing time, t_a for the $Zr_{65}Cu_{27.5}Al_{7.5}$ and $Zr_{65}Cu_{35}$ metallic glasses.

Zr_2Cu (103) with annealing time, t_a at various temperatures for the $Zr_{65}Cu_{27.5}Al_{7.5}$ and $Zr_{65}Cu_{35}$ alloys are shown in Fig. 3. The lattice spacing for the former alloy is larger than that for the latter alloy because Al dissolves in Zr_2Cu substituting with Cu. No significant change in the lattice spacing with annealing time and temperature is seen for these metallic glasses, indicating that the Al content of the Zr_2Cu phase remains under the annealing conditions in the $Zr_{65}Cu_{27.5}Al_{7.5}$ alloy. In order to evaluate the strain factor for line-broadening, Hall's formula [16] is applied for the annealed samples. It is described by

$$B\cos\theta_B = \frac{0.94\lambda}{D_t} + 2\varepsilon\sin\theta_B, \qquad (1)$$

where B is the line-broadening width obtained from half-value width of Zr_2Cu peak, θ_B is Bragg angular, λ is wavelength of X-ray, ε is plastic strain and D_t is true grain size. The D_t is obtained by eliminating the second strain term in Equation 1 and by extrapolating the curve of $B\cos\theta_B$ versus $\sin\theta_B$ to $\theta_B = 0$ [17]. Examples of this exercise for various planes are shown in Fig. 4. The line-broadening data were obtained for $Zr_{65}Cu_{27.5}Al_{7.5}$ annealed at 715 K for 120 s to 240 s and for $Zr_{65}Cu_{35}$ annealed at 645 K for 540 s to 720 s. The linearity is observed for all curves with a slope of approximately 0, indicating that the strain term can be ignored. Therefore, the grain size calculated from the line-broadening of (103) plane can be regarded as a true grain size of Zr_2Cu. Fig. 5 shows the change in the grain size of the $Zr_{65}Cu_{27.5}Al_{7.5}$ and $Zr_{65}Cu_{35}$ alloys with annealing time, t_a. The results obtained by TEM observation are in agreement with those calculated by Scherrer's formula. The change of the grain size with t_a is parabolic, indicating the existence of an exponential functional relation between them. Bright-field TEM images and selected-area electron diffraction patterns of the $Zr_{65}Cu_{27.5}Al_{7.5}$ alloy annealed at 710 K for 150 s (a), (b), 270 s (c), (d) and of the $Zr_{65}Cu_{35}$ alloy annealed at 640 K for 720 s (e), (f), 1020 s (g), (h) are shown in Fig. 6. Very fine crystalline particles in the diameter range from 7 to 18 nm are seen over the whole area of the $Zr_{65}Cu_{27.5}Al_{7.5}$ sample annealed for 150 s. The selected-area electron diffraction pattern corresponds to a Zr_2Cu phase. The ZrAl phase cannot be identified in the limited area because of its small volume fraction. The Zr_2Cu grains grow in the diameter range of approximately 20 nm for the sample annealed for 270 s. The precipitates are also identified as Zr_2Cu. Similarly, it is seen that the grain of the $Zr_{65}Cu_{35}$ alloy increases from 10 nm after 720 s to 20 nm after 1020 s.

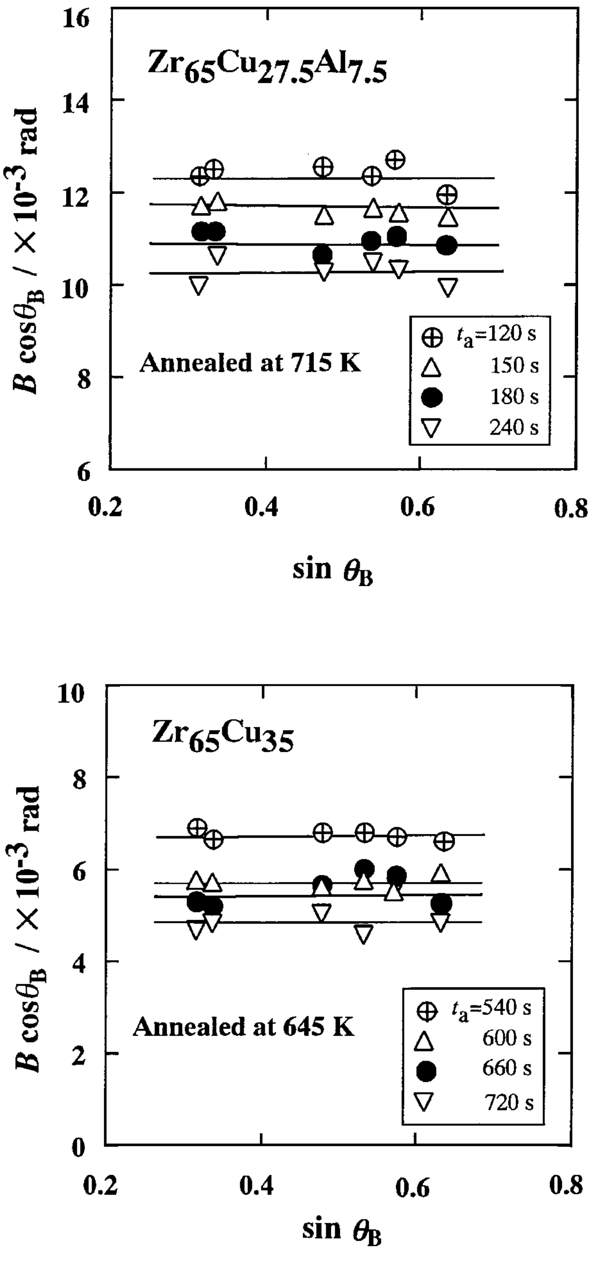

Figure 4 $B\cos\theta_B$ versus $\sin\theta_B$ with various annealing times, t_a for $Zr_{65}Cu_{27.5}Al_{7.5}$ annealed at 715 K and $Zr_{65}Cu_{35}$ annealed at 645 K.

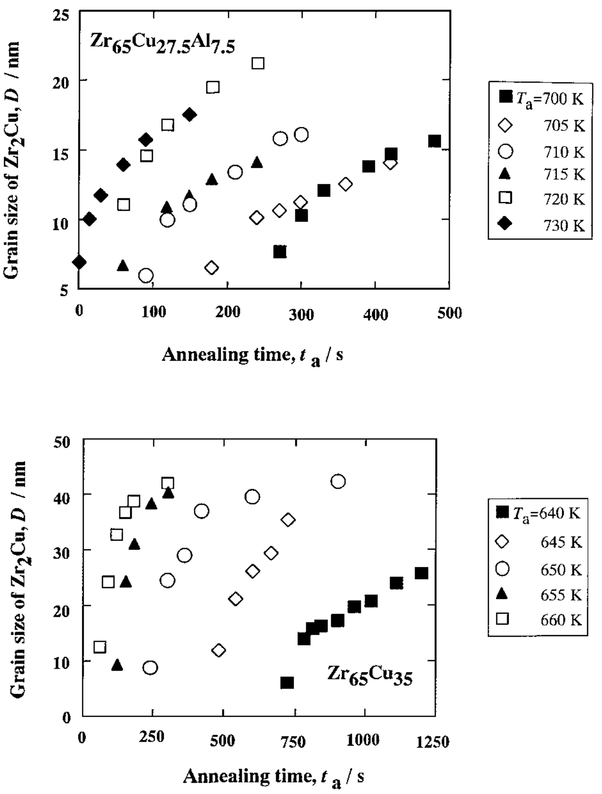

Figure 5 Change in the grain size of Zr_2Cu with annealing time, t_a at various temperatures for the $Zr_{65}Cu_{27.5}Al_{7.5}$ and $Zr_{65}Cu_{35}$ metallic glasses.

Considering the incubation time for grain growth, the growth time, t_g is defined as follows:

$$t_g = t_a - t_0, \tag{2}$$

where t_0 is the time identified from the peak first in the X-ray diffraction pattern during isothermal annealing. Figs 7 and 8 show the change in the grain size and grain growth rate of Zr_2Cu with grain growth time, t_g at various temperatures in the $Zr_{65}Cu_{27.5}Al_{7.5}$ and $Zr_{65}Cu_{35}$ alloys, respectively. The grain size increases monotonously with increasing grain growth time and their size increases with an increase of annealing temperature at the same growth time. For an example, the grain size is approximately 10 nm at 705 K and 18 nm at 720 K for t_g of 100 s. It is due to the difference in the diffusivity among the constituent elements. As shown in Fig. 8, the grain size decreases with increasing growth time. The grain growth rate $\mathrm{d}D/\mathrm{d}t_g$ yields a linear relation with logarithm of t_g as follows:

$$\frac{\mathrm{d}D}{\mathrm{d}t_g} = a - b \log t_g, \tag{3}$$

where a and b are constant.

The Avrami exponent is approximately 3.7 in the supercooled liquid region, implying a constant nucleation rate through an interfacial reaction-controlling process during crystallization in the $Zr_{65}Cu_{27.5}Al_{7.5}$ glassy alloy [13]. The decrease of grain growth rate is originated from the collision among grown crystalline grains, owing to a constant increase in the number of nuclei with increasing annealing time. We can estimate the change in the growth rate with annealing temperature by extrapolating the linear relation between

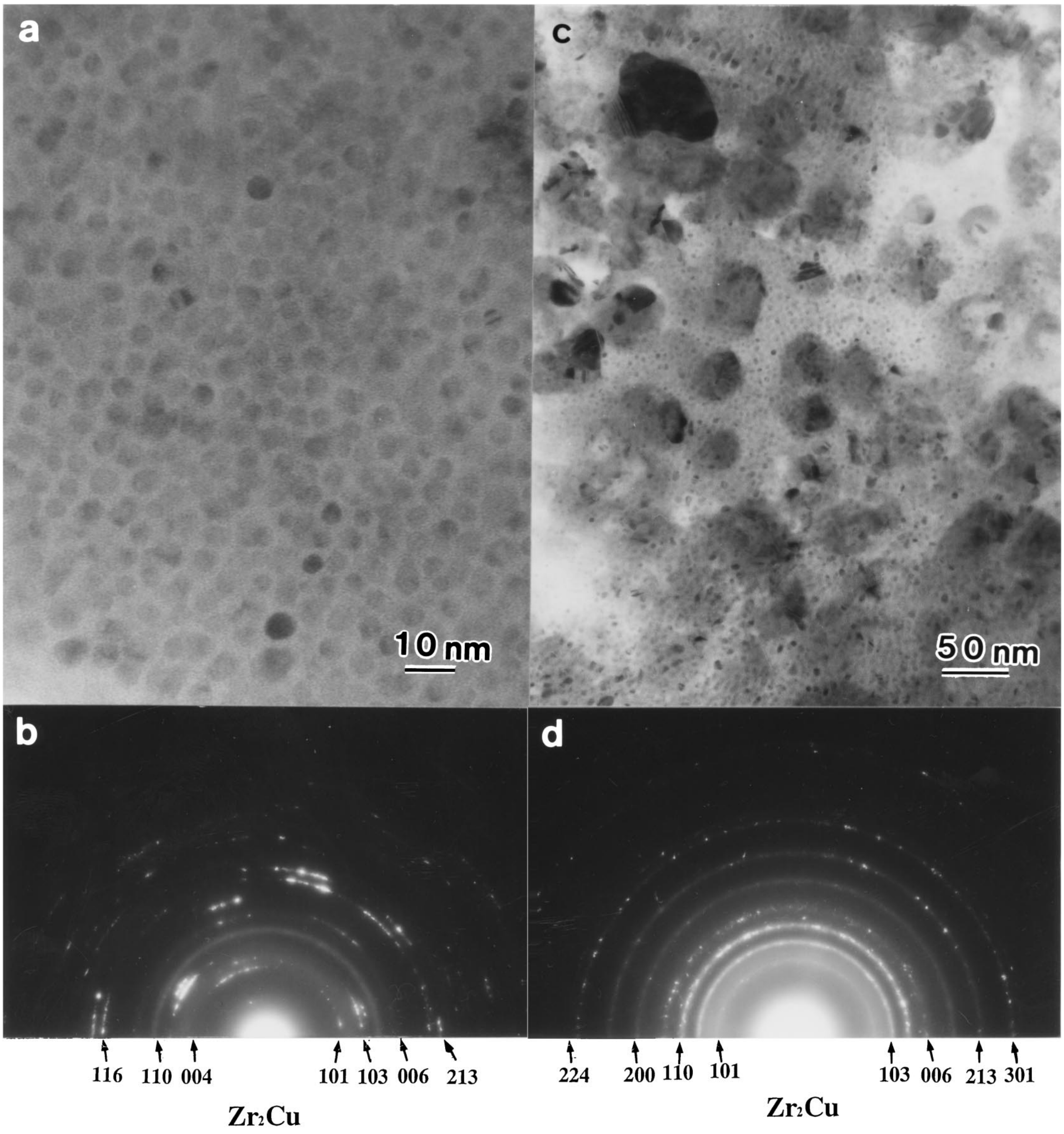

Figure 6 Bright-field electron images and selected area diffraction patterns of $Zr_{65}Cu_{27.5}Al_{7.5}$ annealed at 710 K for 150 s (a), (b), 270 s (c), (d) and $Zr_{65}Cu_{35}$ annealed at 640 K for 720 s (e), (f), 1020 s (g), (h), respectively. (*Continued*)

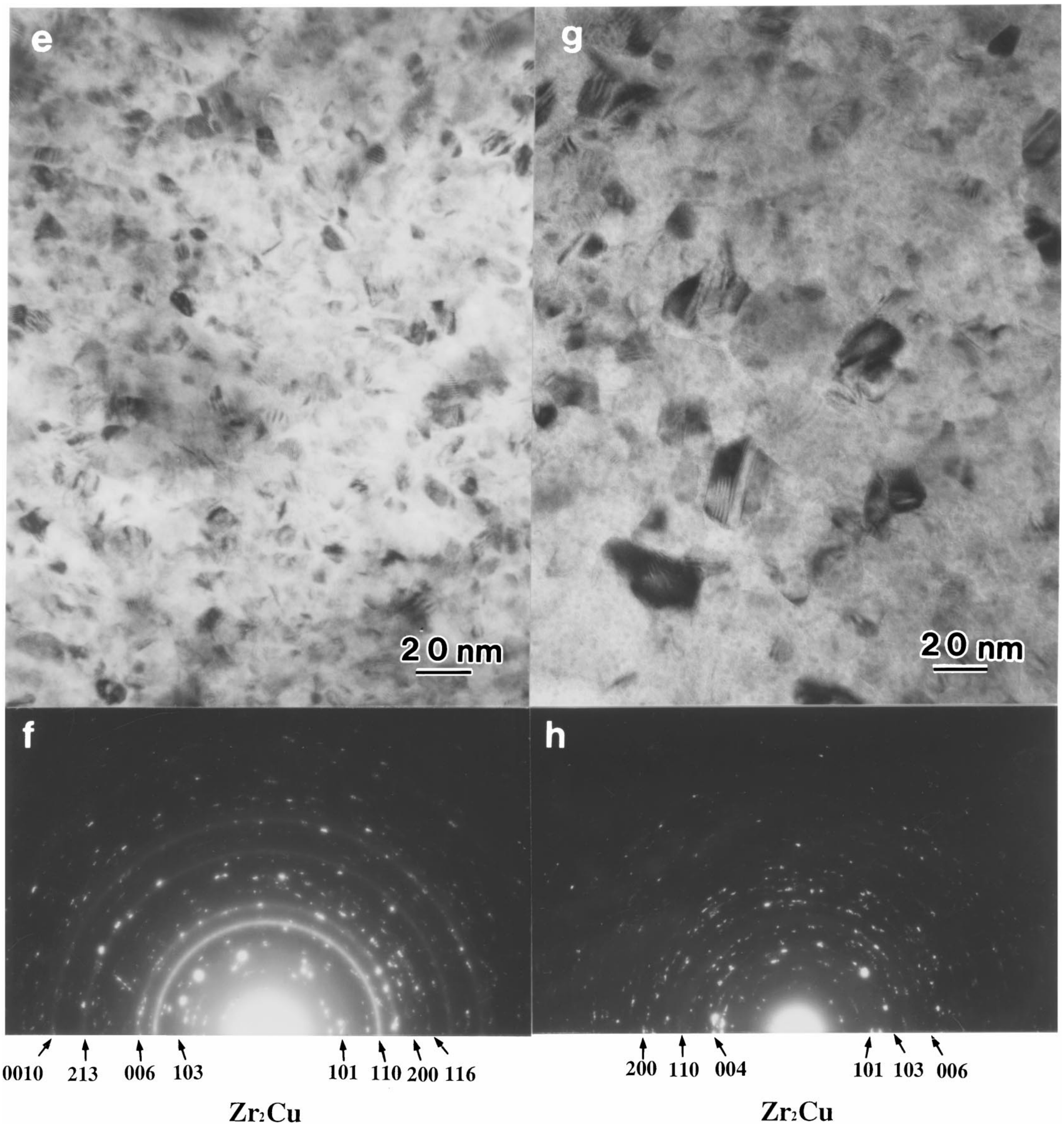

Figure 6 (*Continued*).

$\mathrm{d}D/\mathrm{d}t_\mathrm{g}$ and log t_g. Fig. 9 shows the change in the calculated grain growth rate at $t_\mathrm{g} = 1$ s (i.e. $\log t_\mathrm{g} = 0$) with annealing temperature in the $Zr_{65}Cu_{27.5}Al_{7.5}$ and $Zr_{65}Cu_{35}$ alloys. T_g and T_x of each metallic glass are also shown in this figure. In the $Zr_{65}Cu_{35}$ metallic glass, the growth of Zr_2Cu phase begins at the annealing temperature just over T_g and the growth rate increases suddenly with increasing annealing temperature. On the other hand, the growth rate of Zr_2Cu phase in the $Zr_{65}Cu_{27.5}Al_{7.5}$ alloy is extremely low even at the temperature near T_x. Since the difference in the growth behavior between two metallic glasses is attributed to the difference in the mobility of the constitutional elements, these results indicate that Al restrains the grain growth and nucleation of crystalline phase. While Zr and Cu in the $Zr_{65}Cu_{35}$ alloy can move at the temperature above T_g, the mobility of Cu in the $Zr_{65}Cu_{27.5}Al_{7.5}$ alloy decreases, leading to the formation of primary compound between Al and Zr due to their strong chemical affinity. Therefore, the low growth rate of Zr_2Cu in the $Zr_{65}Cu_{27.5}Al_{7.5}$ alloy is dominated by a necessity of deconvolution of Zr-Al pair. Also the low diffusivity of Al into Zr_2Cu phase substituting with Cu may lead to the low growth rate.

4. Discussion

It has previously been reported [13] that the $Zr_{65}Cu_{27.5}Al_{7.5}$ alloy crystallizes through the polymorphic reaction in which a single crystalline $Zr_2(Cu, Al)$ phase precipitates from the amorphous matrix. However, the authors have pointed out that at the initial crystallization stage, the ZrAl has precipitated as a metastable phase [14]. The formation of the metastable ZrAl phase may be attributed to the difficulty of diffusion of Al to Zr_2Cu resulting from the strong chemical

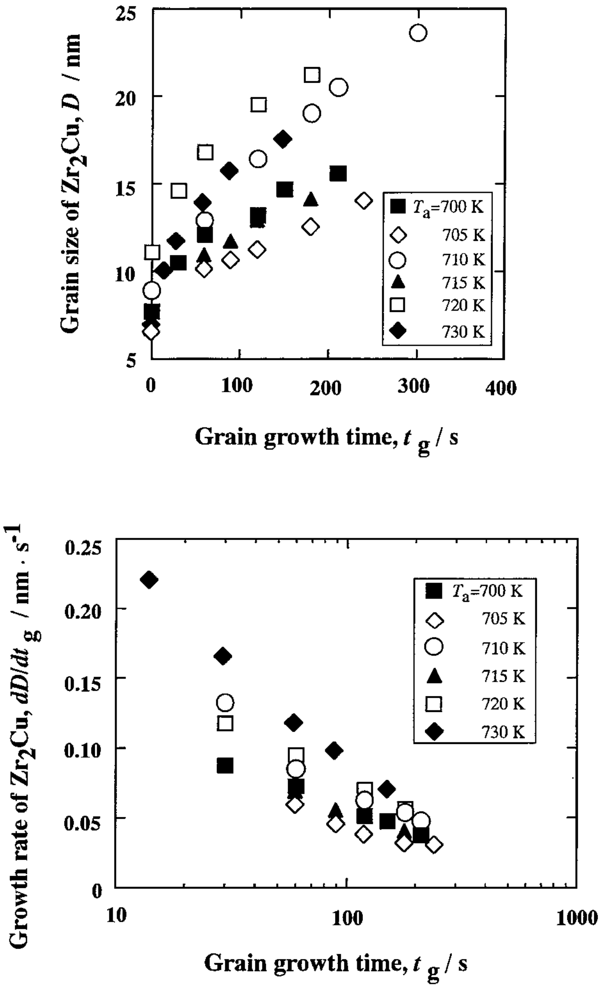

Figure 7 Change in the grain size and grain growth rate of Zr_2Cu with grain growth time, t_g at various temperatures for the $Zr_{65}Cu_{27.5}Al_{7.5}$ metallic glass.

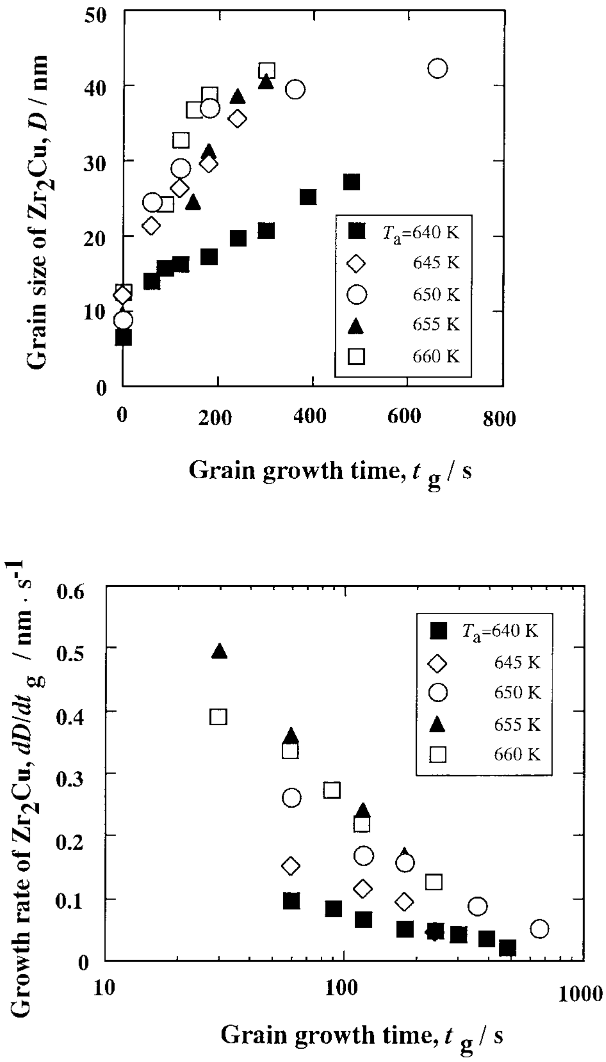

Figure 8 Change in the grain size and grain growth rate of Zr_2Cu with grain growth time, t_g at various temperatures for the $Zr_{65}Cu_{35}$ metallic glass.

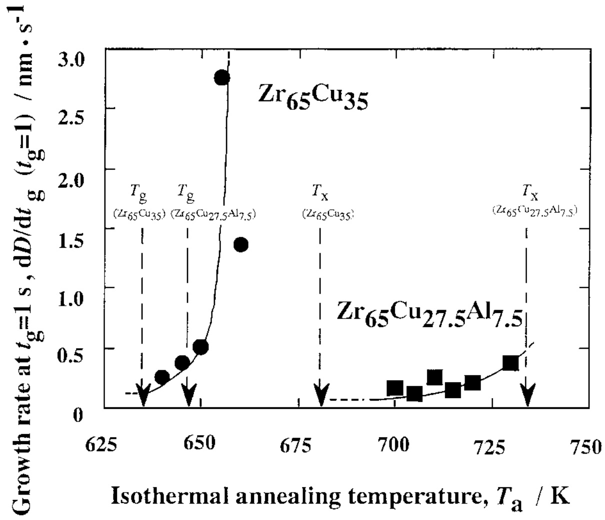

Figure 9 Change in the calculated grain growth rate at $t_g = 1$ s with annealing temperature for the $Zr_{65}Cu_{27.5}Al_{7.5}$ and $Zr_{65}Cu_{35}$ metallic glasses.

affinity between Zr and Al [18], which retards the nucleation of the crystalline phases. From the comparison of grain growth rate in the $Zr_{65}Cu_{27.5}Al_{7.5}$ and $Zr_{65}Cu_{35}$ alloys shown in Fig. 9 it is concluded that the rearrangement of Al restrains the grain growth of crystalline phases. Based on previous works, Inoue has pointed out the importance of two factors of the appearance of such a stable supercooled liquid region [13]. That is, it is presumably due to the suppression of growth reaction resulting from the necessity of long-range redistribution of Al and the difficulty of precipitation of $Zr_2(Cu, Al)$ caused by the high solid-liquid interfacial energy. In the present study, it has been clarified that the rearrangement of Al controls the whole crystallization reaction including the grain growth. The effect of Al on the grain growth is subsequently investigated in comparison with the $Zr_{65}Cu_{35}$ glassy alloy.

The calculated growth rates at $t_g = 1$ s at all temperatures are shown in Fig. 10 in the form of Arrhenius plot, assuming the linearity of growth rate with t_g at the initial stage. The linearity of the Arrhenius plots indicates that the growth rate is given by Equation 4,

$$\frac{\mathrm{d}D}{\mathrm{d}t_g} = u_0 \exp\left(\frac{-Q}{RT}\right). \tag{4}$$

Here, u_0 is the pre-factor, R is gas constant and Q is the activation energy for grain growth. The Q values calculated from the slope of Arrhenius plots are 115 kJ mol^{-1} for $Zr_{65}Cu_{27.5}Al_{7.5}$ and 363 kJ mol^{-1} for $Zr_{65}Cu_{35}$, respectively. This tendency is also seen for the activation energy for crystallization analyzed by

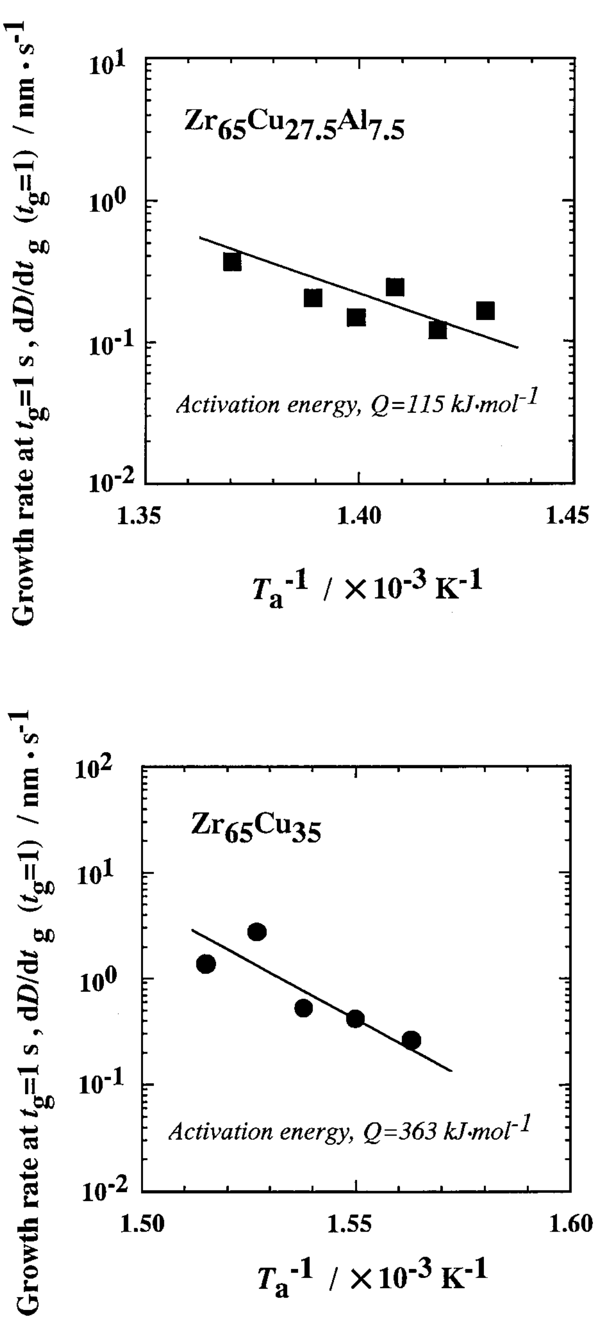

Figure 10 Arrhenius plots of the gain growth rate against reciprocal of annealing temperature for the $Zr_{65}Cu_{27.5}Al_{7.5}$ and $Zr_{65}Cu_{35}$ metallic glasses.

Kissinger plot shown in Fig. 11. The plot of ln (T_p^2/α) versus reciprocal of T_p, where T_p is the peak temperature of crystallization and α is the heating rate, yields a linear relation, from which the activation energy for crystallization is 195 kJ mol^{-1} for $Zr_{65}Cu_{27.5}Al_{7.5}$ and 269 kJ mol^{-1} for $Zr_{65}Cu_{35}$. The difference in the activation energies is explained by the mechanism of grain growth. In the $Zr_{65}Cu_{27.5}Al_{7.5}$ alloy, the grain growth seems to depend on the diffusion or rearrangement of Al. The smaller activation energies of grain growth and crystallization are corresponding to the rearrangement of only Al. In contrast, as the crystallization depends on the rearrangement of both Zr and Cu, much larger activation energies are necessary for crystallization and grain growth in the $Zr_{65}Cu_{35}$ alloy. The large Zr atom needs much larger activation energy [19]. Moreover, the order of magnitude for diffusion in the metallic glasses during grain growth and crystallization reflects the activation energy. Since the precipitation and growth of the crystalline Zr_2Cu phase by diffusing many atoms simultaneously are observed in the $Zr_{65}Cu_{35}$ alloy, the magnitude for diffusion at the initial stage of crystallization is larger than that in the $Zr_{65}Cu_{27.5}Al_{7.5}$ alloy. The formation of ZrAl also plays a role in the barrier for the rearrangement of constitutional elements on a large scale. Thus, the reason for the formation of ZrAl at the initial crystallization stage is presumed to result from the difference in the heat of mixing among the constitutional elements. The calculated heat of mixing of Al and Cu with Zr are −164 kJ mol^{-1} and −78 kJ mol^{-1}, respectively [20]. At the initial crystallization stage, ZrAl as well as Zr_2Cu is formed. The mobility of Al increases with increasing annealing temperature or time, and Al can diffuse into Zr_2Cu by substituting Cu.

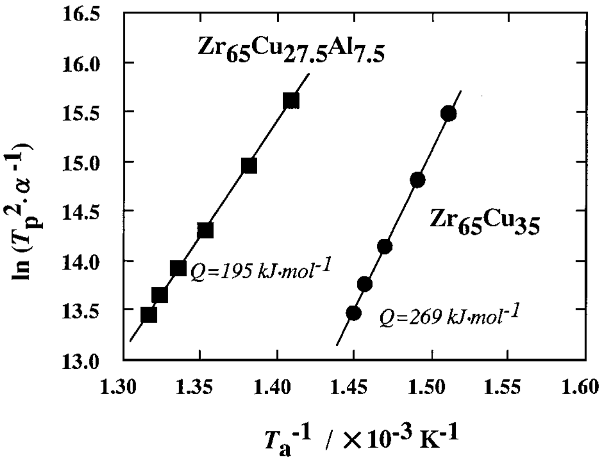

Figure 11 Kissinger plots of the variation of the crystallization peak temperature, T_p with heating rate, α for the $Zr_{65}Cu_{27.5}Al_{7.5}$ and $Zr_{65}Cu_{35}$ metallic glasses.

5. Conclusions

With the aim of investigating the grain growth behavior of a crystalline phase from the supercooled liquid region of the $Zr_{65}Cu_{27.5}Al_{7.5}$ and $Zr_{65}Cu_{35}$ metallic glasses, the change in the grain size was examined as a function of annealing time at various temperatures. The results obtained are summarized as follows:

(1) At the initial stage of crystallization, Zr_2Cu and ZrAl phases are identified in the $Zr_{65}Cu_{27.5}Al_{7.5}$ alloy, in contrast to a single Zr_2Cu phase in the $Zr_{65}Cu_{35}$ alloy. The line-broadening of the X-ray diffraction peak is attributed to only a grain size, resulting from the unchanged lattice spacing during the isothermal annealing and Hall's analysis for various diffraction peaks. The grain size of Zr_2Cu calculated by Scherrer's equation agrees with that obtained by TEM observation.

(2) The relationship between the grain growth rate and logarithm of grain growth time, t_g yields a linear relation, from which the growth rate at $t_g = 1$ s is obtained at all temperatures. The grain growth of Zr_2Cu phase is extremely slow below T_x in the ternary alloy,

while the grain in the binary alloy grows rapidly just above T_g and its growth rate is much larger.

(3) The activation energy for the grain growth of Zr_2Cu is 115 kJ mol^{-1} for $Zr_{65}Cu_{27.5}Al_{7.5}$ and 363 kJ mol^{-1} for $Zr_{65}Cu_{35}$. The same tendency is recognized in the activation energy for crystallization evaluated by Kissinger plot. The small activation energy for $Zr_{65}Cu_{27.5}Al_{7.5}$ is attributed to the mechanism of which the crystallization and grain growth are dominated by the redistribution of only Al. It is concluded that the strong chemical affinity between Al and Zr retards the formation and growth of Zr_2Cu phase, which is an important factor of stabilizing the glassy state.

References

1. A. INOUE, K. OHTERA, K. KITA and T. MASUMOTO, *Jpn. J. Appl. Phys.* **27** (1988) L2248.
2. S. G. KIM, A. INOUE and T. MASUMOTO, *Mater. Trans. JIM.* **31** (1990) 929.
3. A. INOUE, H. YAMAGUCHI, T. ZHANG and T. MASUMOTO, *ibid.* **31** (1990) 104.
4. H. S. CHEN, *Rep. Prog. Phys.* **3** (1980) 353.
5. A. INOUE, K. AMIYA, I. YOSHII, N. NISHIYAMA and T. MASUMOTO, *Mater. Sci. Eng.* **A179/180** (1994) 692.
6. A. INOUE, T. ZHANG and T. MASUMOTO, *Mater. Trans. JIM.* **31** (1990) 177.
7. T. ZHANG, A. INOUE and T. MASUMOTO, *ibid.* **32** (1991) 1005.
8. A. INOUE, T. ZHANG and T. MASUMOTO, *J. Non-Cryst. Solids* **150** (1992) 396.
9. H. SCHUMACHER, U. HERR, D. OELGESCHLAEGER, A. TRAVERSE and K. SAMWER, *J. Appl. Phys.* **82** (1997) 155.
10. R. RAMBOUSKY, M. MOSKE and K. SAMWER, *Z. Phys.* **B99** (1996) 387.
11. D. KAWASE, A. P. TSAI, A. INOUE and T. MASUMOTO, *Appl. Phys. Lett.* **62** (1993) 137.
12. A. P. TSAI, D. KAWASE, A. INOUE and T. MASUMOTO, in Proceedings of the 6th Topical Meeting on Crystal Growth Mechanism, Awara, January 1992, p. 421.
13. A. INOUE, D. KAWASE, A. P. TSAI, T. ZHANG and T. MASUMOTO, *Mater. Sci. Eng.* **A178** (1994) 255.
14. J. SAIDA, M. MATSUSHITA, K. YAOITA and A. INOUE, *Mater. Trans. JIM.* **40** (1999) 1117.
15. B. D. CULLITY, "Elements of X-ray Diffraction" 2nd ed. (Addison Wesley Pub. Co., Mass., 1978) p. 84.
16. W. H. HALL, *J. Inst. Met.* **75** (1950) 1127.
17. K. ISONISHI and K. OKAZAKI, *J. Mater. Sci.* **28** (1993) 3829.
18. E. MATSUBARA, T. TAMURA, Y. WASEDA, A. INOUE, T. ZHANG and T. MASUMOTO, *Mater. Trans. JIM.* **33** (1992) 873.
19. U. KÖSTER, J. MEINHARDT, S. ROOS and H. LIEBERTZ, *Appl. Phys. Lett.* **69** (1996) 179.
20. A. K. NIESSEN, F. R. DE BORE, R. BOOM, P. F. DE CHÂTEL, W. C. M. MATTENS and A. R. MIEDEMA, *CALPHAD* **7** (1983) 51.

Received 19 May 1999
and accepted 3 February 2000